Investigation of Energy Transfer between CdTe Nanocrystals on Polystyrene Beads and Dye Molecules for FRET-SNOM Applications†

Felix Müller,‡ Stephan Götzinger,‡ Nikolai Gaponik,§ Horst Weller,§ Jürgen Mlynek,‡ and Oliver Benson*,‡

Institute of Physics, Nano-Optics, Humboldt-University Berlin, Hausvogteiplatz 5-7, D-10117 Berlin, Germany, and Institute of Physical Chemistry, University of Hamburg, D-20146 Hamburg, Germany

Received: February 23, 2004; In Final Form: May 24, 2004

We report results on the observation of energy transfer between CdTe nanocrystals and AlexaFluor dye molecules. The nanocrystals were attached to the surface of polystyrene latex beads of 450 nm in diameter by means of the layer-by-layer technique. Energy transfer was observed as signal enhancement in confocal imaging of a single bead covered with an AlexaFluor film. This was verified by detecting quenching of the donor emission and enhancement of the acceptor emission in spectral measurements. A fluorescence-resonance energy transfer scanning near-field optical microscopy (FRET-SNOM) tip was made from a single bead coated with CdTe attached to a near-field tip. We report first results on FRET-SNOM imaging with this tip.

Introduction

One of the main goals in modern optical microscopy is to obtain atomic resolution. However, the Abbe diffraction limit defines a boundary that cannot be overcome in usual wide-field imaging microscopy where propagating fields are collected. As early as 1928, Synge[1] proposed the idea of scanning near-field optical microscopy (SNOM), which was only realized in 1984 by Pohl.[2] The new approach in SNOM is to use local scattering of nonpropagating evanescent fields into propagating fields which then can be collected by ordinary optics. The resolution limit in this method is given only by the size of the local scatterer. SNOM has been used in a great number of different configurations.[3] One possible classification is to divide aperture SNOM from apertureless SNOM. The first kind is most similar to Synge's original idea: A sample is illuminated via a light source behind a tiny, subwavelength aperture. Nowadays, this aperture is realized by tapered and metal-coated fiber tips.[2,4] If this aperture is scanned across a sample by using scanning techniques similar to scanning tunneling microscopy or atomic force microscopy (AFM), the nonpropagating field at the aperture is scattered into propagating modes. By monitoring the scattered light, an image can be reconstructed with subwavelength resolution which is determined by the size of the aperture. Unfortunately, this size is not defined by the physical dimensions of the aperture but rather by the skin depth of the metal used to make the aperture. The skin effect limits the resolution to about 30 nm.[5] In apertureless SNOM, different approaches have been demonstrated to overcome this limitation. For example, in scanning photon tunneling microscopy,[6] a very small uncoated tip, or even an AFM tip,[7] locally scatters the evanescent fields from an illuminated sample. Also local field enhancement by the nanometer-sized tip[8] or illumination by using a nanoscopic light source down to a single molecule[9] have been used to obtain subwavelength optical resolution. All these methods have their own advantages and disadvantages, respectively.

The smallest feature in a SNOM image is given by a convolution of the shape of the tip with the real feature on the sample. If there is a strong nonlinear dependence of the scattering process on the tip-to-sample distance, then the resolved size of the features can be significantly reduced. Thus, scattering processes with a very strong nonlinear dependence are desirable in order to improve the resolution in SNOM imaging. In a similar way, nonlinear effects are also used in fluorescence confocal optical microscopy to reduce the effective spot size.[10]

A well-studied process that can be exploited for this purpose is fluorescence (or Förster) resonant energy transfer[11] (FRET) between fluorophores, for example, dye molecules. In FRET, an excited donor molecule can transfer its energy to an acceptor molecule directly via dipole−dipole interaction. The transfer rate k is described by the Förster rate equation[12]

$$k = \frac{1}{\tau_D}\left(\frac{R_0}{r}\right)^6 \qquad {R_0}^6 = 8.758 \times 10^{-5}\,\frac{\kappa^2 \phi_D J}{n^4}$$

In this formula, τ_D is the donor lifetime in the absence of the acceptor, r is the donor−acceptor distance, and R_0 is the so-called Förster radius. The Förster radius is related to a factor κ^2 which accounts for the dipole orientation of the donor relative to the acceptor. Finally, Φ_D is the quantum yield of the donor, n the index of refraction and J an overlap integral that quantifies the spectral overlap between the donor's emission spectrum and the acceptor's absorption spectrum. The characteristic length scale, the Förster radius R_0, is between 1 and 8 nm,[11] depending on the FRET pair. Because the strong distance dependence (the transfer rate is inversely proportional to the sixth power of the distance between donor and acceptor), FRET has been used as a molecular "ruler" to determine small distances on a molecular scale.[13] FRET can be detected by measuring the quenching of the emission of the donor or by an enhancement of the emission of the acceptor. Modifications of the decay of the fluorescence from the donor have been studied as well.[14] Many applications

† Part of the special issue "Gerhard Ertl Festschrift".

* To whom correspondence may be addressed. E-mail: oliver.benson@physik.hu-berlin.de.

‡ Humboldt-University Berlin.

§ University of Hamburg.

10.1021/jp049183s CCC: $27.50
Published on Web 07/01/2004

have been demonstrated in ensemble and even single molecule measurements (see ref 15 and references therein). Recently, it has also been speculated to use FRET in artifical materials in order to engineer the energy flow.[16]

In particular, for the application of FRET in single molecule spectroscopy, it is desirable to work with a very stable and efficient donor−acceptor pair. The use of inorganic−organic hybride systems made from a semiconductor nanoparticle and an organic dye molecule has recently attracted much attention. Colloidally synthesized semiconductor nanocrystals[17] (NCs) have unique optical and spectroscopic properties that possess several inherent advantages over organic dyes. They provide a large photoluminescence quantum yield, their emission spectrum is narrow, and they can be tuned over a wide region of the optical spectrum by changing the nanocrystal size or material composition. The latter property allows an easy way of fine tuning of the overlap of the donor emission and the acceptor absorption, respectively, in a FRET pair. Finally, the broad absorption band of NCs provides convenient excitation, e.g., by a simple UV lamp. The development of several methods to disperse NCs in aqueous solution opened the way to applications in a biologically relevant environment.[18] In several experiments, it has been demonstrated that NCs can replace dye molecules as donors.[19] Moreover, NCs and organic molecules have been assembled in order to realize smart biosensors.[20]

In this paper, we concentrate on a different application, where the inorganic and organic fluorophores do not form a coupled hybride pair, but are manipulated individually. Sekatskii et al.[21] proposed to use the FRET mechansim to improve the resolution in SNOM. In the so-called FRET-SNOM, a tip is functionalized with, e.g., donor molecules. By scanning this tip across a sample that is labeled with acceptor molecules and detecting the FRET signal, an improved resolution is expected. First experiments have been performed that show the feasibility of FRET-SNOM.[22] However, several problems occur. First, the tip has to be scanned across the sample with a distance not exceeding the Förster radius which requires mechanically stable tips. Second, the small active volume of the tip containing the donor is subject to rapid photobleaching. Finally, a tip of well-characterized shape has to be functionalized in a reproducible and reliable way. While writing this paper, it has come to our attention that Ebenstein et al. have recently used CdSe/ZnS nanocrystals bound to the surface of an AFM tip as a possible FRET-SNOM tip.[23] However, it was found that the AFM tip was easily contaminated by acceptor molecules, which were collected when scanning the tip in the required small distance across a sample.

In this paper, we investigated a donor−acceptor pair which tackles the problems mentioned above. As a donor, we chose small polystyrene beads of a few hundred nanometers in diameter which were coated with CdTe nanocrystals.[24] A dye molecule with a suitable absorption spectrum (AlexaFluor 633, Molecular Probes) was used as acceptor. We provide first studies of this novel donor−acceptor pair and demonstrate how it can be used in a reliable and well-defined FRET-SNOM configuration. Our system allows a much more stable scanning operation compared to what has been demonstrated so far. After a description of the experimental setup, we report measurements of the spectral properties of the donor and acceptor, respectively, and show results on FRET interaction. Then, we describe how we assemble our FRET-SNOM tips. Finally, we give first evidence for successful FRET microscopy. We conclude with a discussion of further improvements of our FRET-SNOM system.

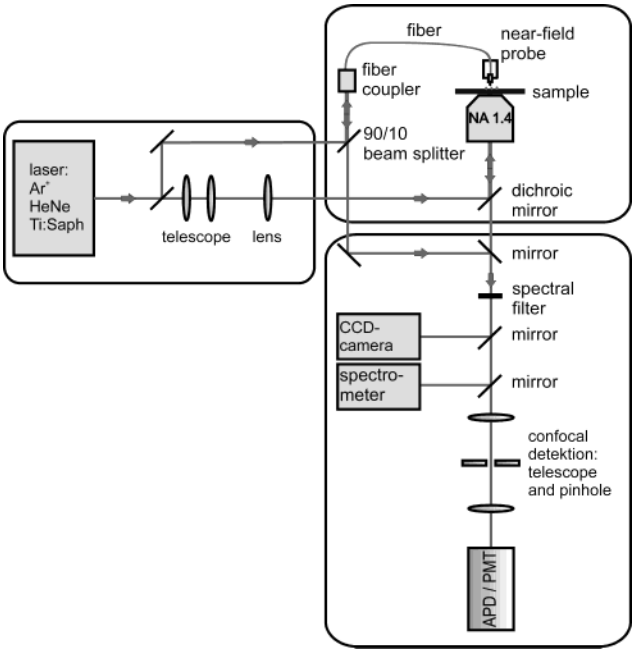

Figure 1. Schematic of the experimental setup. The sample is mounted on a $x-y$ scanner on an inverted confocal microscope. Different lasers can be used for excitation. Filtering and subsequent detection of the fluorescence via different ports (CCD camera, spectrometer, confocal detection) are possible. A near-field microscope can be attached for high-resolution measurements and FRET-SNOM measurements on the sample.

Experimental Methods

Setup. A schematic of the experimental setup is shown in Figure 1. It consists of a home-made inverted scanning confocal optical microscope. Light from different laser sources (Ar^+−ion laser, He−Ne laser, Ti−sapphire laser) was focused by a high-NA microscope objective (NA = 1.4) on the sample. The sample could be scanned with nanometer precision in $x-y$ direction using a piezoelectric scanner. The focus was adjusted by moving the mount of the microscope objective in the z direction with a piezo. Fluorescence light was separated from the pump light by a dichroic mirror and several optical filters. Alternatively, the dichroic mirror could be replaced by a 90/10 beam splitter. The sample was inspected by an eyepiece or a sensitive CCD camera in wide-field mode or the detected light was focused on a pinhole and directed to an avalanche photodiode (APD, dark-count rate $< 80\ s^{-1}$), a photomultiplier, or a spectrometer (resolution 0.2 nm). The setup can be combined with a home-made near-field optical microscope.[25]

The flexibility of the setup allows to study various samples. As an example, parts a and b of Figure 2 show a confocal image of single red-emitting dye molecules (DiI, Molecular probes). The scan area was $10 \times 10\ \mu m^2$, and pump light from the Ar^+−Ion laser ($\lambda = 514$ nm) at an intensity of 1600 W/cm^2 was used. A similar confocal image was taken from a sample where CdSe nanocrystals with a ZnS shell[26] were spin coated on a cover slip (Figure 2c). The fluorescence maximum is around 620 nm, the density is about 30−50 NC per 100 μm^2, and the excitation source was again an Ar^+−ion laser ($\lambda = 514$ nm) at an intensity of 3600 W/cm^2. An intensity profile along the line indicated by the arrows is plotted as well in Figure 2d (top). The full width at half maximum of the intensity profile from a single NC defines the resolution of our system, which was 240 nm and thus slightly larger than what is theoretically expected[27] (for this wavelength, 160 nm are predicted). The setup allows

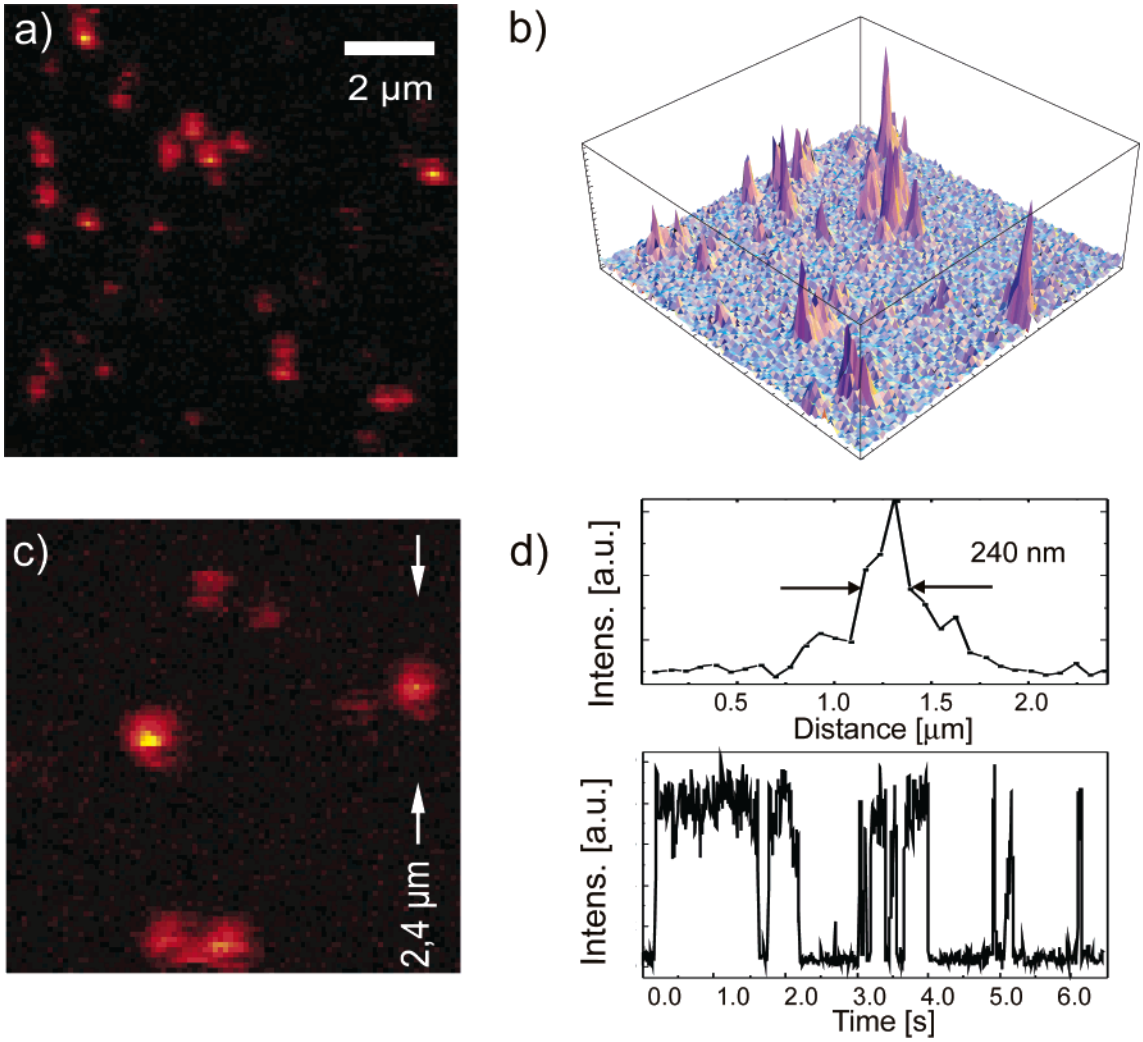

Figure 2. Confocal image of the fluorescence from individual spin-coated DiI molecules (a and b) and CdSe/ZnS nanocrystals (c) under excitation with $\lambda = 514$ nm. The top figure in part d is an intensity cross-section along the line indicated in part c. The bottom figure in part d is a time trace of the fluorescence from a single nanocrystal measured by an avalanche photodiode that shows the pronouced blinking behavior of a single nanocrystal.

also to study the time dependence of the fluorescence from a single NC by sending the light on the APD. Figure 2d (bottom) shows the intensity of the emission from a single NC. A random intermittence of the intensity is clearly observed. This so-called "blinking" phenomenon is a well-known property of nanocrystals.[28] The abrupt jumps between an "on" and an "off" state can be used as a fingerprint for emission from a single emitter. Thus, the intensity profile shown in Figure 2d results indeed from a pointlike source and provides the spatial resolution of our system directly.

Materials. In our experiments, we studied dye molecules and colloidally synthesized semiconductor nanocrystals.[17] As pointed out in the Introduction, NCs with tailored surface properties and sufficiently strong luminescence offer many advantages compared to dye molecules. They provide higher stability and a tunability via changing the particle's size or material composition. Furthermore, they have a large absorption cross section and a wide absorption band. For all of the following experiments, we used CdTe nanocrystals.

CdTe NCs capped by thioglycolic acid were synthesized in aqueous solution according to a previously published procedure.[24] Size-selective precipitation[24] was applied to the crude solution of NCs to select the strongly emitting fraction with a photoluminescence maximum at around 620 nm, which was used for further investigations.

For FRET applications, the emission spectrum of the donor fluorophor and the absorption spectrum of the acceptor fluorophor have to be matched. In a real application, the quenching of the donor emission and the enhancement of the acceptor emission is only a gradual effect. The remaining emission of the donor has to be separated by the acceptor emission by careful filtering. A compromise between a good overlap between donor emission and acceptor absorption on one hand and a sufficient separability between donor and acceptor emission on the other hand has to be found. After studying different samples, we chose the dye molecule AlexaFluor 633 (Molecular Probes) as the acceptor together with the CdTe NCs as the donor. Figure 3a shows the measured emission spectrum of the CdTe NCs (red curve, confocal excitation with 80 W/cm^2 at $\lambda = 476$ nm), a measured emission spectrum of a thin film of AlexaFluor 633 (black curve, confocal excitation with 800 W/cm^2 at $\lambda = 476$ nm), and the excitation spectrum of AlexaFluor 633 (blue curve, data provided by Molecular Probes). From an observation of the spectra, it is apparent that there is a good overlap of the donor emission (CdTe NC, red curve) and the acceptor absorption (AlexaFluor 633, blue curve). At the same time, by setting a filter with a cutoff at around 640 nm, it is possible to block the remaining donor fluorescence. We chose an excitation wavelength of $\lambda = 476$ nm for our experiments. Figure 3b shows the absorption spectrum of the CdTe NCs (red curve) and

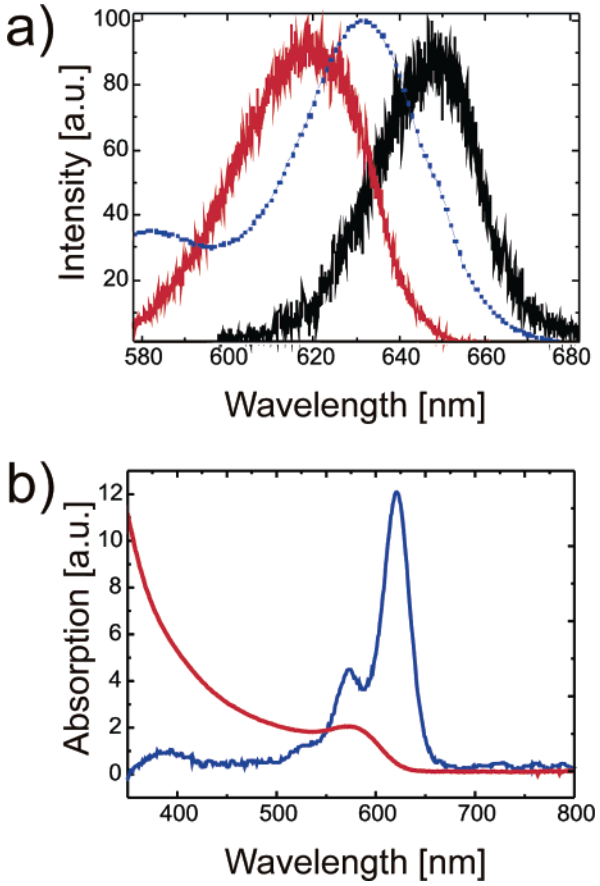

Figure 3. (a) Measured emission spectrum of the CdTe NCs (red curve), measured emission spectrum of a thin film of AlexaFluor 633 (black curve), and the excitation spectrum of AlexaFluor 633 (blue curve, data provided by Molecular Probes). (b) Absorption spectrum of CdTe NCs (red curve) and AlexaFluor 633 (blue curve). At the excitation wavelength of $\lambda = 476$ nm, the absorption efficiency of AlexaFluor is below 1% of the maximum value.

AlexaFluor 633 (blue curve). At this wavelength, the absorption of AlexaFluor is below 1% of its maximum value, whereas the absorption of the CdTe NCs is already large. This is also reflected by the 1 order of magnitude higher excitation intensity for AlexaFluor compared to CdTe when the spectra in Figure 3a were taken. Thus, at this wavelength, direct excitation of AlexaFluor is (not completely but strongly) suppressed. From an inspection of the spectra, it is evident that for the purpose of FRET applications NCs provide ideal donors: They have a clean emission spectrum that can be tuned at will to match a certain acceptor molecule. Additionally, they can always be excited with high efficiency far from the acceptor absorption.

Results

Evidence for FRET by Confocal Measurements. As pointed out in the Introduction, one problem in FRET-SNOM is to make functionalized probes in a reproducible way. A well-defined nanoscopic probe can be produced by beads that are coated with active material. Polystyrene latex beads are commercially available in sizes ranging from several micrometers to below 100 nm and have a very well-defined smooth surface and reproducible shape (The size distribution is less than 3%). If such a bead is attached to a scanning tip, e.g., a SNOM or AFM tip, then a reliable and robust probe is formed. The production of such probes will be described below. Here, we propose to use NCs as active material for the coating.

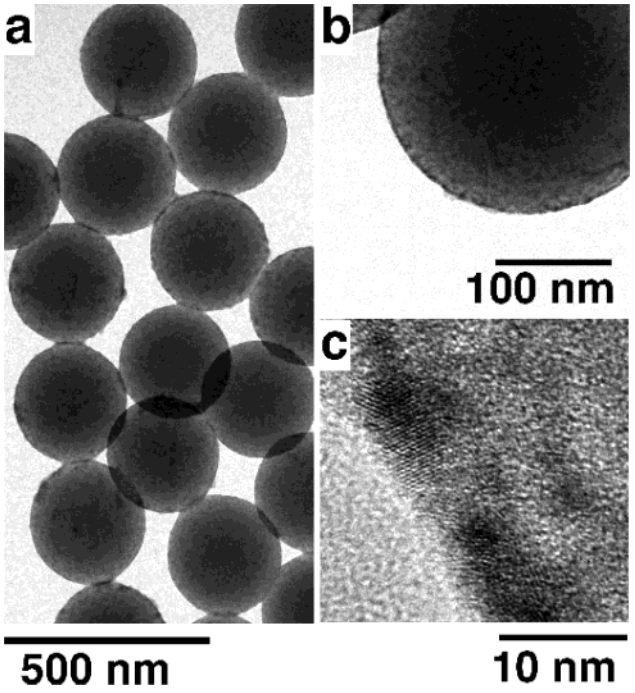

Figure 4. TEM and high-resolution TEM images of CdTe nanocrystals on polystyrene beads with increasing resolution from part a to part c. The efficient coverage of the beads with nanocrystals can be clearly seen in part c, where the crystal structure of individual nanocrystals is resolved.

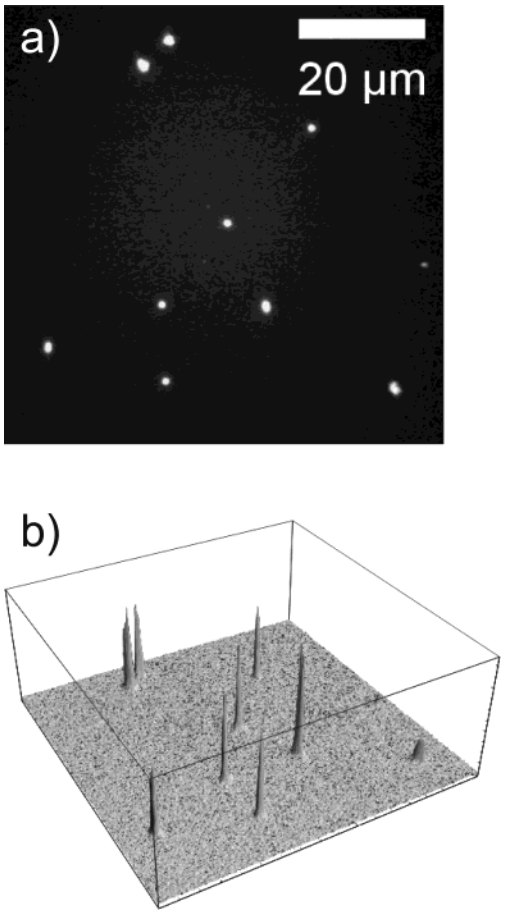

Figure 5. Wide-field image of a sample of spin-coated beads of a diameter of 450 nm covered with CdTe nanocrystals. The constant height of the intensity peaks show that there is no agglomeration of the beads.

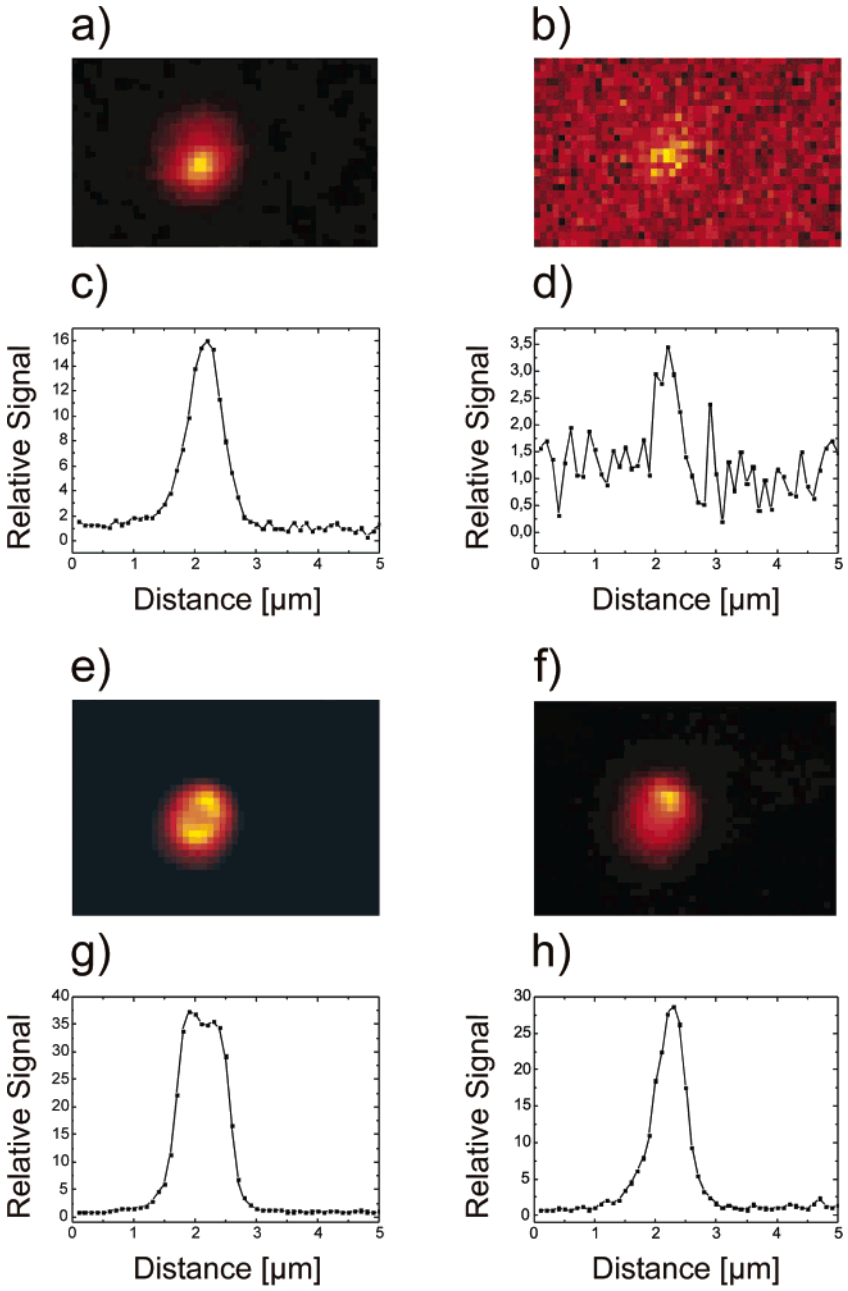

Figure 6. Confocal images and intensity cross sections of a single bead of 450 nm in diameter. Measurements in parts a−d were with an uncoated bead (CdTe-coated sample); the measurements in parts e−h, the bead was covered with AlexaFluor molecules (CdTe/AF-coated sample). Each set of measurements was performed with a green filter (in a and c and e and g) as well as with a red filter (in b and d and f and h). The red filter blocks light from the NCs (donor) and transmits light mainly from the AlexaFluor molecules (acceptor).

Colloidally synthesized NCs have successfully been used for the fabrication of shells on colloidal particles.[29] In particular, polystyrene latex beads can be coated with CdTe NCs by means of the layer-by-layer technique.[30] Beads of 270 and 450 nm were purchased from Duke Scientific, California. The layer-by-layer technique was used to modify the surface of the beads. The procedure was as follows: the beads were subsequently covered with the positive polyelectrolyte (polyallylamine hydrochloride, PAH, MW $\approx$ 50 000), followed by negative polyelectrolyte (polystyrene sulfonate, PSS, MW $\approx$ 70 000) and again with positive PAH. Finally, the negatively charged[24] CdTe NCs were adsorbed on the bead's surface. The beads were carefully washed after each covering step by multiple centrifugation/redispersion in water. The last redispersion was done in absolute ethanol to achieve uniform drying of the sample on a cover slip before optical measurements were undertaken. Figure 4 shows high-resolution transmission electron microscopy (TEM) images of modified beads, confirming the efficient (almost 100%) coverage of the bead's surface with CdTe NCs.

After the coating of the beads, the luminescent properties were studied. Figure 5 shows a wide-field image of a few beads of a diameter of 450 nm (excitation with 64 W/cm^2 at $\lambda = 514$ nm) that were spin coated on a cover slip. The bright spots all have the same intensity, which proves that there is no agglomeration of the beads. This was confirmed by imaging the topography of the sample with the SNOM. The measurement of the spectrum of CdTe shown in Figure 3 was actually from CdTe NCs on these beads.

First evidence for energy transfer from the CdTe coated beads to the AlexaFluor acceptor is given by confocal measurements. We produced two different samples. One sample (denoted CdTe-coated sample) was similar to the one shown in Figure 5 where

the beads were spin coated on a cover slip. On the other sample (denoted CdTe/AF-coated), the beads were spin coated and subsequently drop cast with a layer of AlexaFluor 633. The procedure produced a film with homogeneous optical thickness which was checked by scanning the areas under investigation with a He−Ne laser at $\lambda = 633$ nm as the excitation source. As is evident from Figure 3b, the He−Ne laser only excites the AlexaFluor molecules and not the CdTe NCs. Confocal measurements were then performed by using two different filters for the fluorescence light: a green filter (transmission > 95% above 550 nm) and a red filter (transmission > 95% above 647 nm). Both filters suppressed the transmission below the cutoff wavelength by a factor of 10^{-5}. Comparison with the measured emission spectrum of the donor and acceptor (Figure 3a) reveals that the green filter transmits both the acceptor and donor emission, whereas the red filter blocks most of the fluorescence from the donor. Both filters also block the excitation light, which was at a wavelength of 476 nm and an intensity of 470 W/cm^2.

Figure 6 shows the experimental results for measurements on the CdTe-coated sample (parts a−d) and the CdTe/AF-coated sample (parts e−h). A two-dimensional confocal image of a single bead and a one-dimensional cut in the *x* direction through the region of highest intensity is plotted. In the measurement with the CdTe-coated sample, the maximum relative intensity (the background noise was normalized to 1 in the measurements) drops to 17% when switching from the green filter (a and c) to the red filter (b and d). In the CdTe/AF-coated sample, however, the decrease in intensity was only down to 76%. This gives strong evidence that energy transfer from the CdTe coated bead occurs to the AlexaFluor molecules around the bead. In the measurement with the red filter, mostly light from the acceptor is detected. In the ideal case, there should be no detectable signal in parts b and d of Figure 6. The remaining signal arises from nonperfect blocking of the donor emission by the filter. We would like to stress that there was no effect merely by agglomeration of the AlexaFluor around the beads. We checked this by exciting the coated probe with a He−Ne laser at $\lambda = 633$ nm, which did not excite the CdTe coated beads but only the AlexaFluor molecules. No enhanced emission from AlexaFluor due to agglomeration around the beads was observed in these measurements.

To verify that energy transfer occurred in the NC−AlexaFluor molecule system, we performed spectral measurements on a single bead. Figure 7 shows the measured spectra when a single CdTe-coated bead which was covered with a layer of AlexaFluor was confocally excited by the Ar^+−ion laser at a wavelength of $\lambda = 476$ nm and an intensity of 800 W/cm^2 (blue curve). Comparison with Figure 3a reveals that the measured spectrum contains the fluorescence from both the CdTe NCs and the AlexaFluor molecules. The red curve is a measurement of a spectrum which was performed under exactly the same excitation conditions but after the AlexaFluor had been bleached by intense (100 kW/cm^2) light from the He−Ne laser at $\lambda = 633$ nm. As mentioned above, the NCs could not be excited by the He−Ne laser and were thus not affected. We checked this by a control experiment on a sample containing only CdTe NCs. The emission spectrum and intensity after illumination by the He−Ne laser did not change. A striking difference to the blue curve is the enhanced emission around 620 nm and the reduced emission at 640 nm. These wavelengths correspond to the maxima of the NCs and the AlexaFluor emission, respectively. The measurement thus shows that one criterium for energy transfer is observed: when the acceptor molecules (AlexaFluor) are present, then the donor (CdTe NCs) emission is strongly

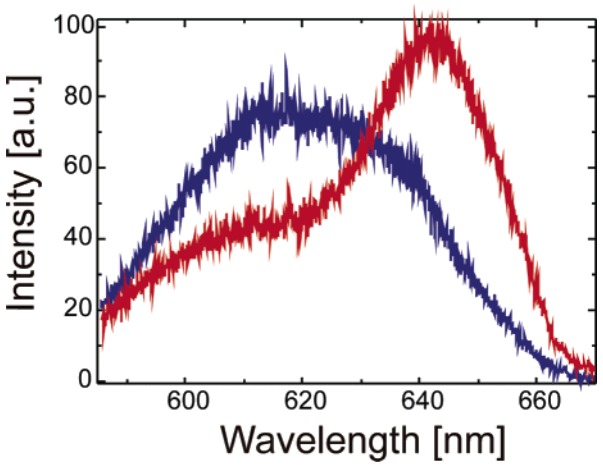

Figure 7. Measured spectra from a single bead covered with a homogeneous layer of AlexFluor. The red curve was measured after the AlexaFluor had been photobleached by an intense He−Ne laser. An enhanced emission around 620 nm (donor emission) and a reduced emission at 640 nm (acceptor emission) is clearly visible after photobleaching.

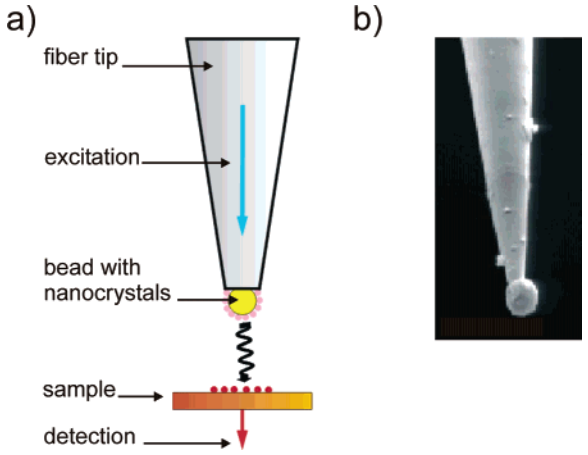

Figure 8. (a) Schematic of an application of CdTe coated beads in FRET-SNOM: A single bead with the NCs as donors is attached to a SNOM tip and scanned across a sample which is labeled with acceptor molecules. The enhanced acceptor emission is detected to obtain an image with improved sub-wavelength resolution. (b) SEM image of a single bead of approximately 500 nm in diameter attached to a near-field probe.

quenched. At the same time, an enhancement of acceptor emission is observed. From the measurement, it is possible to derive a value of 40% for the FRET efficiency, which is the ratio of the integrated donor intensity with and without the presence of the acceptor.[31] This value gives an upper limit to the efficiency and assumes that the whole surface of the bead is covered with acceptor molecules. It is, however, similar to recent results obtained in ref 22.

Measurements with FRET-SNOM Tips. The clear evidence of energy transfer in a system involving polystyrene beads of 450 nm in size that were coated with NCs is very promising for FRET-SNOM applications. Figure 8a shows a schematic of a FRET-SNOM, where a single bead is attached to a SNOM tip. It has been demonstrated[32] that single nanoparticles of a few hundred nanometers down to at least 50 nanometers can be attached in a setup where an inverted confocal microscope is combined with a SNOM, very similar to our case. Probes with attached beads subdivide the technological difficulty to make both a robust (the tip has to be scanned very close to the surface) and a functionalized scanning tip in two independent

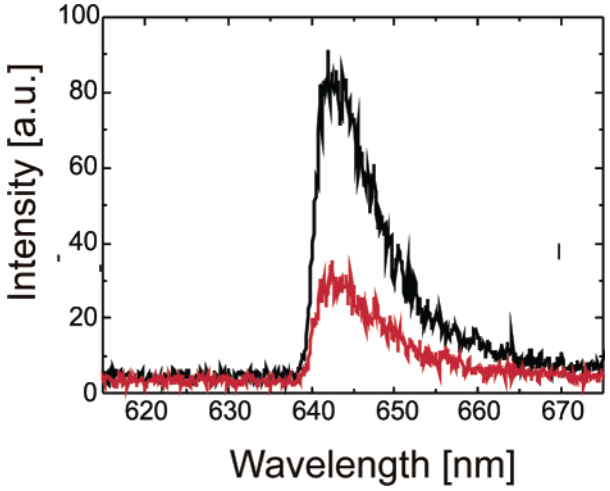

Figure 9. Measured spectra taken via the microscope objective when the FRET-SNOM tip was approximately 15 nm away from the sample (normal shear-force regime, red curve) and less than or equal to 3 nm away from the sample (strong damping regime, black curve), respectively. The sharp cutoff at the high energy side is due to a red filter, which was used to block the remaining donor emission.

problems. The well-known shape of the tip apex (formed by the bead) also faciliates to recognize topological artifacts[33] in FRET-SNOM images. Because of the pronounced nonlinear behavior of the FRET signal from the distance between the bead and the acceptor molecules, the possible resolution is much smaller than the size of the bead. It is possible to define a FRET-SNOM aperture with a simple geometrical estimation: Only NCs on the bead which are within a distance of the Förster radius from the probe contribute to the FRET signal. Thus, a cut through the bead at a distance R_0 from the bead's surface determines the effective aperture radius R_a, which for a bead with radius r is given by the following expression

$$R_a = (2rR_0 - R_0^2)^{1/2}$$

For a bead with a radius of 50 nm and a Förster radius of 4 nm, this would result in a value of $R_a = 20$ nm, which is comparable to the best reported values of the resolution of aperture SNOM.[5]

Figure 8b shows an SEM image of a FRET-SNOM tip where a single bead of approximately 500 nm in diameter is attached to a SNOM tip. A similar tip coated with CdTe was mounted in our SNOM in order to perform first tests of FRET-SNOM imaging. We drop cast a thin film of AlexaFluor 633 on a cover slip in the sample holder of the confocal microscope. The distance between the FRET-SNOM tip and the surface of the cover slip was actively controlled by using a shear-force control loop common in scanning near-field optical microscopy.[34] The shear-force distance control relies on the mechanical interaction of an oscillating fiber tip with a surface. When the fiber tip approaches the surface, the oscillation is damped. This provides a signal for a feedback loop. In this way, we can hold or scan the tip at a well-defined separation. We distinguished two regimes, namely, the strong damping and the normal shear-force regime. In the first regime, the tip−sample separation was less than or equal to 3 nm, whereas in the normal shear-force regime, it was approximately 15 nm. Figure 9 shows spectra taken via the microscope objective when the FRET-SNOM tip was in

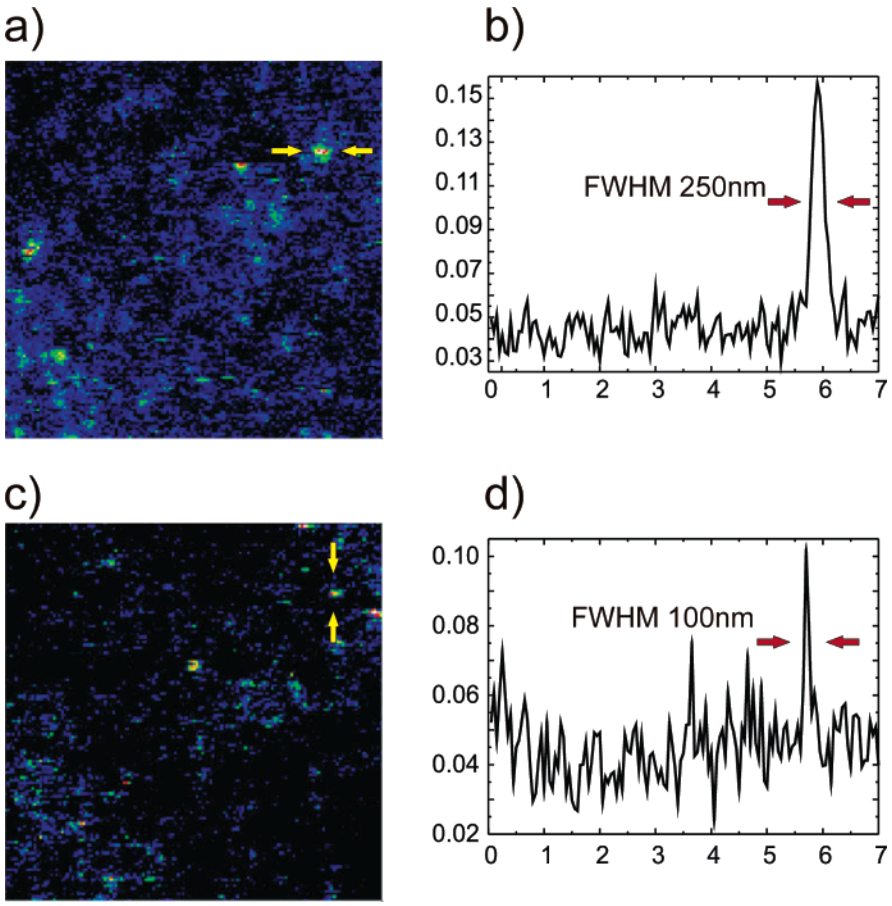

Figure 10. FRET-SNOM image of a sample with a dilute film of AlexaFluor 633. An area of 7 μm × 7 μm was scanned at a scanning rate of 2 μm/s in the normal shear force (a) and strong damping regime (c), respectively. Parts b and d show intensity profiles through the structures indicated by arrows.

the normal shear-force regime (red curve) and in the strong damping regime (black curve), respectively. The spectra were taken with the red filter which accounts for the sharp cutoff at the high energy side. A pronounced enhancement of emission at longer wavelengths is clearly visible when the FRET-SNOM tip is within a distance comparable to the Förster radius. This gives strong evidence that energy transfer from the CdTe donors to AlexaFluor acceptor molecules occurred. A remarkable feature of our FRET-SNOM system is that the tip could be scanned in the strong damping regime, i.e., at a distance of less or equal than 3 nm at a scanning rate of 5−10 μm/s.

To demonstrate that imaging is possible, we scanned an area of a sample that we drop cast with a very dilute solution of Alexa Fluor (10−50 molecules per 100 μm^2). Figure 10 shows two areas of 7 μm × 7 μm on the sample scanned in the normal shear-force (Figure 10a) and strong damping regime (Figure 10c), respectively. Parts b and d of Figure 10 show intensity profiles through characteristic structures which result from small agglomerates of AlexaFluor molecules. In the normal shear-force regime, the most narrow widths of the intensity profiles we found were on the order of the resolution of a confocal scan (250 nm), whereas in the strong damping regime, we found widths as narrow as 100 nm. These results give evidence that indeed an enhanced resolution was obtained due to the FRET mechanism.

Discussion and Conclusion

We have analyzed energy transfer between polystyrene beads coated with CdTe as donors and AlexaFluor molecules as acceptors. We observed efficient FRET in confocal and spectral measurements and demonstrated the operation of a FRET-SNOM made from a single bead attached to a near-field probe. Distance-dependent measurements gave further evidence for the onset of energy transfer from CdTe nanocrystals to AlexaFluor molecules. The stable and repeatable scanning mode has the potential to extend the method toward single-molecule imaging. By attaching smaller beads to the tip (the attachment of 50 nm beads has been demonstrated already), a resolution of 10 nm or below is within reach. The results demonstrate that our system is a very promising candidate for FRET-SNOM applications or for studying controlled interaction between nanocrystals and single molecules.

Acknowledgment. We thank Andreas Kornowski for taking the TEM images and A. Eychmüller and Dmitri Talapin, University of Hamburg, T. Kalkbrenner, S. Kühn, V. Sandoghdar, ETH Zurich, and A. Rogach, University of Munich, for fruitful collaboration and discussion. This work was partially funded by DFG Grant BE2224/4.

References and Notes

(1) Synge, E. H. *Philos. Mag.* **1928**, *6*, 356.
(2) Pohl, D. W.; Denk, W.; Lanz, M. *Appl. Phys. Lett.* **1984**, *44*, 651.
(3) Paesler, M. A.; Moyer, P. J. In *Near-field Optics: Theory, Instrumentation and Applications*; Wiley: New York 1996.
(4) Lewis, A. Isaacson, M.; Harootunian, A.; Murray, A. *Ultramicroscopy* **1984**, *13*, 227.
(5) Liebermann, K.; Harush, S.; Lewis, A.; Kopelman, R. *Science* **1990**, *247*, 59. (b) Nowotny, L.; Pohl, D. W.; Hecht, B. *Opt. Lett.* **1995**, *20*, 970.
(6) Reddick, R. C.; Warmack, R. J.; Ferrell, T. L. *Phys. Rev. B* **1989**, *39*, 767. (b) Courjon, D.; Sarayeddine, K.; Spajer, M. *Opt. Comm.* **1989**, *71*, 23.
(7) Zenhausen, F.; O'Boyle, M. P.; Wickramasinghe, H. K. *Appl. Phys. Lett.* **1994**, *65*, 1623.
(8) Novotny, L.; Sánchez, E. J.; Xie, X. S. *Ultramicroscopy* **1998**, *71*, 21.
(9) Michaelis, J.; Hettich, C.; Mlynek, J.; Sandoghdar, V. *Nature* **2000**, *405*, 325.
(10) Dyba, M.; Hell, S. W. *Phys. Rev. Lett.* **2002**, *88*, 163901.
(11) Wu, P.; Brand, L. *Anal. Biochem.* **1994**, *218*, 1.
(12) Förster, T. In *Modern Quantum Chemistry*; Sinanoglu, O., Ed.; Academic Press: New York, 1965; Vol. III, pp 93−137, .
(13) Stryer, L. *Annu. Rev. Biochem.* **1999**, *47*, 819−846 (1078); some applications can also be found in the special issue *Science* **283**, No. 5408.
(14) Lakowicz, J. R. In *Principles of Fluorescence Spectroscopy*; Plenum Press: New York, 1983.
(15) Jares-Erijman, E. A.; Jovin, T. M. *Nature Biotech.* **2003**, *21*, 1387.
(16) Crooker, S. A.; Hollingsworth, J. A.; Tretiak, S.; Klimov, V. I. *Phys. Rev. Lett.* **2002**, *89*, 186802.
(17) Murray, C. B.; Norris, D. J.; Bawendi, M. G. *J. Am. Chem. Soc.* **1993**, *115*, 8706. (b) Empedocles, S. A.; Neuhauser, R.; Shimizu, K.; Bawendi, M. G. *Adv. Mater.* **1999**, *11*, 1243. (c) Alivisatos, A. P. *Pure Appl. Chem.* **2000**, *72*, 3−9. (d) Gaponenko, S. V. *Optical Properties of Semiconductor Nanocrystals*; Cambridge University Press: Cambridge, 1998.
(18) Bruchez, M.; Moronne, M.; Gin, P.; Weiss, S.; Alivisatos, A. P. *Science* **1998**, *281*, 2013−2015.
(19) Clapp, A. R.; Medintz, I. L.; Mauro, J. M.; Fisher, B. R.; Bawendi, M. G.; Mattoussi, H. *J. Am Chem. Soc.* **2004**, *126*, 301−310.
(20) Chan, W. C.; Nie, S. *Science* **1998**, *281*, 2016−2018. (b) Mattoussi, H.; Kuno, M. K.; Goldman, E. R.; Anderson, G. P.; Mauro, J. M. In *Optical Biosensors: Present and Future*; Elsevier: Amsterdam, 2002; pp 537. (c) Medintz, I. L.; Clapp, A. R.; Mattoussi, H.; Goldman, E. R.; Fisher, B.; Mauro, J. M. *Nature Materials* **2003**, *2*, 630.
(21) Sekatskii, S. K.; Lethokov, V. S. *Appl. Phys. B. Opt. Laser* **1996**, *63*, 525.
(22) Vickery, S. A.; Dunn, R. S. *J. Microsc.* **2001**, *202*, 408. (b) Shubeita, G. T.; Sekatskii, S. K.; Dietler, G.; Letokhov, V. S. *Appl. Phys. Lett.* **2002**, *80*, 2625. (c) Shubeita, G. T.; Sekatskii, S. K.; Dietler, G.; Potapova, I.; Mews, A.; Basché, T. *J. Microsc.* **2003**, *210*, 274.
(23) Ebenstein, Y.; Mokari, T.; Banin, U. *J. Phys. Chem. B* **2004**, *108*, 93.
(24) Gaponik, N.; Talapin, D. V.; Rogach, A. L.; Hoppe, K.; Shevchenko, E. V.; Kornowski, A.; Eychmüller, A.; Weller, H. *J. Phys. Chem.* **2002**, *106*, 7177.
(25) Details of the SNOM setup can be found in: Götzinger, S.; Benson, O.; Sandoghdar, V. *Appl. Phys. B* **2001**, *73*, 825.
(26) Talapin, D. V.; Rogach, A. L.; Kornowski, A.; Haase, M.; Weller, H. *Nano Lett.* **2001**, *1*, 207.
(27) Webb, R. H. *Rep. Prog. Phys.* **1996**, *59*, 427.
(28) Neuhauser, R. G.; Shimitzu, K. T.; Woo, W. K.; Empedocles, S. A.; Bawendi, M. G. *Phys. Rev. Lett.* **2000**, *85*, 3301.
(29) Caruso, F. *Adv. Mater.* **2001**, *13*, 11.
(30) Susha, A. S.; Caruso, F.; Rogach, A. L.; Sukhorukov, G. B.; Kornowski, A.; Möhwald, H.; Giersig, M.; Eychmüller, A.; Weller, H. *Colloids Surf. A* **2000**, *163*, 39.
(31) Ha, T.; Enderle, T.; Ogletree, D. F.; Chemla, D. S.; Selvin, P. R.; Weiss, S. *Proc. Natl. Acad. Sci. U.S.A.* **1996**, *93*, 624.
(32) Kalkbrenner, T.; Ramstein, M.; Mlynek, J.; Sandoghdar, V. *J. Microsc.* **2001**, *202*, 72.
(33) Greffet, J. J.; Carminati, R. *Prog. Surf. Sci.* **1997**, *56*, 133.
(34) Barenz, J.; Hollrichter, O.; Marti, O. *Rev. Sci. Instrum. 6* **1996**, *7*, 1912.